Journal of Statistical Physics, Vol. 114, Nos. 1/2, January 2004 (© 2004)

Numerical Integration of a Non-Markovian Langevin Equation with a Thermal Band-Passing Noise

Jing-Dong Bao[1]

Received December 12, 2002; accepted June 6, 2003

An accurate and fast approach for numerically solving a non-Markovian Langevin equation with a thermal band-passing noise is proposed. The algorithm combines the closed integration for both damping and noise terms with the Runge–Kutta method for nonlinear force in the Markovian Langevin equation transferred from the original equation. The present algorithm is tested through simulating diffusion of a free particle by using different initial distributions, and then a strong superdiffusion is shown. The mean velocity of a particle in a flashing ratchet driven by the band-passing colored noise is calculated numerically. The dependence of the resulting mean velocity on temperature, asymmetry of the ratchet potential, and inertia of the particle is discussed, and some novel behaviors in comparison with the usual model are observed.

KEY WORDS: Band-passing noise; non-Markovian Langevin equation; strong superdiffusion; flashing ratchet.

1. INTRODUCTION

In recent years, growing attention has been focused on the processes that take place in disordered media and systems that show anomalous diffusive behaviors.[1] The dynamical origin of the anomalous diffusion is due to the nonlocality in time and thus the velocity of the particle has a memory effect, resulting in a non-Markovian Langevin equation (NMLE).[2–4] Morgado *et al.*[5] modified the noise density of states of the thermal bath

[1] Department of Physics, Beijing Normal University, Beijing 100875, People's Republic of China; e-mail: jdbao@bnu.edu.cn

0022-4715/04/0100-0503/0 © 2004 Plenum Publishing Corporation

by removing the lower part of the acoustic modes; thus a deep superdiffusion is observed. Superdiffusion has been found in a number of systems,[6] ranging from early discoveries in intermittent chaotic systems to fluid particles in fully developed turbulence and to millennial climate changes. Nevertheless, a practical example of noise-induced superdiffusion is lacking.

In ref. 7, we presented an external broadband colored noise determined by the difference between two Ornstein–Uhlenbeck noises with different time constants and used it as a nonequilibrium fluctuation source to drive a correlation ratchet.[8] The results have shown that the flux direction of the particle induced by the "green" noise[9] is opposite to the one induced by the usual "red" noise. In this paper, we study the characteristic behaviors of the band-passing noise used as a thermal or inertial noise, namely, the noise and the damping kernel obey the fluctuation-dissipation theorem. An accurate and fast algorithm is developed for simulating the NMLE with the band-passing noise. The proposed thermal band-passing noise is applied to a flashing ratchet and the mean velocity of the particle is calculated numerically.

2. MODEL AND ALGORITHM

2.1. Thermal Band-Passing Noise

The NMLE for the coordinate of a particle in a potential U reads

$$m\ddot{x}(t)+m\int_0^t \beta(t-t')\,\dot{x}(t')\,dt'+U'(x)=\varepsilon(t), \tag{1}$$

where $\beta(t)$ is the friction memory kernel and $\varepsilon(t)$ is a thermal colored noise that we assume to be zero centered, stationary and obeying the fluctuation-dissipation theorem: $\langle \varepsilon(t)\,\varepsilon(t')\rangle = k_B T\beta(|t-t'|)$, where k_B is the Boltzmann constant and T is the absolute temperature of the environment.

As a practical and realizable case of noise-induced superdiffusion, we report on the thermal band-passing colored noise $\varepsilon(t)$ appearing in Eq. (1), which allows a transition between low-passing "red" noise and high-passing "green" noise.[9] It associates with a memory kernel as

$$\beta(t-t')=\frac{\beta_0\tau_1^2}{(\tau_1^2-\tau_2^2)}\left[\frac{1}{\tau_2}\exp\left(-\frac{|t-t'|}{\tau_2}\right)-\frac{1}{\tau_1}\exp\left(-\frac{|t-t'|}{\tau_1}\right)\right], \tag{2}$$

where β_0 is the friction coefficient and τ_1 and τ_2 are two time parameters of the noise. The spectral density of the band-passing noise is given by

$$S(\omega) = \frac{2\beta_0 k_B T \tau_1^2 \omega^2}{(1+\tau_1^2\omega^2)(1+\tau_2^2\omega^2)}. \tag{3}$$

This spectrum shows a broad band and has high frequencies richer than that of the harmonic noise. When $\tau_1 \to \infty$, $S = 2\beta_0 k_B T(1+\tau_2^2\omega^2)^{-1}$ is the "red" spectrum, and when $\tau_2 \to 0$, $S = 2\beta_0 k_B T(\tau_1\omega)^2/(1+\tau_1^2\omega^2)$ has the behavior of the "green" spectrum, which is a constant spectrum of the white noise plus a low-passing spectrum of the "red" noise.

2.2. The Algorithm

If one uses a direct numerical integration[10] to solve the NMLE (1), a double-integration for memory velocity needs to be performed, i.e.,

$$\int_t^{t+\Delta t} dt' \int_0^{t'} \beta(t-s)\, v(s)\, ds = \sum_{k=0}^{n-1} \beta([n-k]\,\Delta t)\, v(k\,\Delta t)(\Delta t)^2, \tag{4}$$

and the integration for random force $\Gamma_n = \int_{n\,\Delta t}^{(n+1)\,\Delta t} \varepsilon(s)\, ds$ needs to be simulated, where Δt is the time step. The variance $\langle \Gamma_n^2 \rangle$ can be evaluated easily from the correlation function of the noise (2). However, the above simulation for the noise should not give the characteristic behaviors of colored noise such as relaxation and selection of frequency. Therefore, one must first use a white noise to produce the colored noise needed. The remaining task is to make the Euler method for nonlinear force valid to order Δt. It is noted that this algorithm requires a long run time and thus should not be recommended.

The present noise defined by the correlation function (2) and the spectrum (3) can proceed from the difference between two Ornstein–Uhlenbeck noises driven by the same white noise $\eta(t)$;

$$\begin{aligned} \varepsilon(t) &= \varepsilon_2(t) - \varepsilon_1(t), \\ \dot{\varepsilon}_i(t) &= -\frac{1}{\tau_i}\varepsilon_i(t) + \frac{1}{\tau_i}\eta(t), \quad (i=1,2), \\ \langle \eta(t) \rangle &= 0, \qquad \langle \eta(t)\,\eta(t') \rangle = 2D\delta(t-t'), \end{aligned} \tag{5}$$

where $D = \beta_0 k_B T[\tau_1/(\tau_1-\tau_2)]^2$. The solution of ε_i reads

$$\varepsilon_i(t) = \varepsilon_i(0)\exp(-t/\tau_i) + \frac{1}{\tau_i}\int_0^t \exp[-(t-s)/\tau_i]\,\eta(s)\, ds. \tag{6}$$

The correlation function of the noise is given by

$$\begin{aligned}\langle \varepsilon(t)\,\varepsilon(t')\rangle = &\sum_{i=1}^{2}\left[\langle \varepsilon_i^2(0)\rangle - \frac{D}{\tau_i}\right]\exp\left(-\frac{t+t'}{\tau_i}\right)\\ &+\left[\langle \varepsilon_1(0)\,\varepsilon_2(0)\rangle - \frac{2D}{\tau_1+\tau_2}\right]\\ &\times\left[\exp\left(-\frac{t}{\tau_1}-\frac{t'}{\tau_2}\right)+\exp\left(-\frac{t}{\tau_2}-\frac{t'}{\tau_1}\right)\right]+k_B T\beta(|t-t'|). \qquad (7)\end{aligned}$$

In order to yield stationary correlation of the noise, i.e., $\langle \varepsilon(t)\,\varepsilon(t')\rangle$ depends only on $|t-t'|$ and is independent of times t and t', we let the former three terms in the r.h.s. of Eq. (7) vanish, leading to $\langle \varepsilon_i(0)\,\varepsilon_j(0)\rangle = 2D/(\tau_i+\tau_j)$ $(i, j = 1, 2)$. Thus, the Gaussian distributions for initial values $\varepsilon_1(0)$ and $\varepsilon_2(0)$ are obtained and simulated as

$$\begin{aligned}\varepsilon_1(0) &= \frac{\tau_1}{\tau_1-\tau_2}\sqrt{\frac{\beta_0 k_B T}{\tau_1}}\,\omega_{10},\\ \varepsilon_2(0) &= \frac{\tau_1}{\tau_1-\tau_2}\sqrt{\frac{\beta_0 k_B T}{\tau_2}}\left[\frac{2\sqrt{\tau_1\tau_2}}{\tau_1+\tau_2}\,\omega_{10}+\frac{\tau_1-\tau_2}{\tau_1+\tau_2}\,\omega_{20}\right],\end{aligned} \qquad (8)$$

where ω_{10} and ω_{20} are two independent normal Gaussian random numbers with zero-mean and variance one.

Now we transfer Eq. (1) into a set of MLE by introducing two variables

$$\begin{aligned}y_1(t) &= A\int_0^t \frac{1}{\tau_1}\exp\left(-\frac{t-s}{\tau_1}\right)\dot{x}(s)\,ds-\varepsilon_1(t),\\ y_2(t) &= -A\int_0^t \frac{1}{\tau_2}\exp\left(-\frac{t-s}{\tau_2}\right)\dot{x}(s)\,ds+\varepsilon_2(t),\end{aligned} \qquad (9)$$

where $A = \beta_0\tau_1^2/(\tau_1^2-\tau_2^2)$. Thus, a MLE with four variables is written as

$$\begin{aligned}\dot{x} &= v(t),\\ m\dot{v} &= f(x)+y_1(t)+y_2(t),\\ \dot{y}_1 &= -\frac{1}{\tau_1}y_1(t)+\frac{A}{\tau_1}v(t)-\frac{1}{\tau_1}\eta(t),\\ \dot{y}_2 &= -\frac{1}{\tau_2}y_2(t)-\frac{A}{\tau_2}v(t)+\frac{1}{\tau_2}\eta(t),\end{aligned} \qquad (10)$$

where $f(x) = -U'(x)$.

A comprehensive approach is proposed here by using a closed integration[11, 12] for both damping and noise terms, combined with the Runge–Kutta method[13] for nonlinear force. The present algorithm is precessed by

$$x(t+\Delta t) = x(t) + \frac{\Delta t}{2}\,[v(t) + v^*(t)], \tag{11}$$

$$v(t+\Delta t) = v(t) + \frac{1}{m}\left\{\int_t^{t+\Delta t} f(x(s))\,ds + \sum_{i=1}^{2}\int_t^{t+\Delta t} y_i(s)\,ds\right\}, \tag{12}$$

$$y_i(t+\Delta t) = \exp\left(-\frac{\Delta t}{\tau_i}\right) y_i(t) + \frac{(-1)^i}{\tau_i}\int_t^{t+\Delta t} \exp\left(-\frac{t+\Delta t-s}{\tau_i}\right) \cdot [-Av(s) + \eta(s)]\,ds \qquad (i = 1, 2). \tag{13}$$

If the potential force is approximately a linear function, $\int_t^{t+\Delta t} f(x(s))\,ds = f(x(t))\,\Delta t$; otherwise, $\int_t^{t+\Delta t} f(x(s))\,ds = [f(x(t)) + f(x^*(t))]\,\Delta t/2$ in general. Here the quantities taking "*" used in multi-step simulation are calculated by the Euler algorithm of Eqs. (10). Four Gaussian random numbers will be needed in each step for the comprehensive algorithm. Namely, the integrations of noise can be simulated by linear combinations of four normal Gaussian random numbers, and matrix elements of the coefficients are evaluated by self- and cross-correlations of the integrations of noise in Eqs. (12) and (13).[14, 15] Nevertheless, if the noise is not in the region of white noise limit and the damping is not too large, all equations in (10) can be simulated well by using the second-order Runge–Kutta method, which needs only one Gaussian random number in each step.

3. RESULTS AND DISCUSSION

We can solve exactly the NMLE (1) when $U = 0$ by using the Laplace transform technique. The asymptotical expression of the mean-square displacement of the particle is obtained as

$$\lim_{t\to\infty} \langle[\Delta x(t)]^2\rangle = k_B T\left\{2\frac{(\tau_1+\tau_2)\,\kappa^2}{(1+\kappa)^3}\,t + \frac{\kappa}{(1+\kappa)^2}\,t^2 - \frac{\kappa^2(\tau_1+\tau_2)^2}{(1+\kappa)^4}\right\}, \tag{14}$$

where $\kappa = \beta_0\tau_1^2/(\tau_1+\tau_2)$. This is called the ballistic diffusion, a strong superdiffusion. It is found that $\lim_{t\to\infty}\langle[\Delta x(t)]^2\rangle = 2k_BT/(m\beta_0)\,t$ for $\tau_1 \to \infty$ and $\tau_2 = 0$. If $\tau_2 \to 0$ only, the noise becomes a "green" noise, $\lim_{t\to\infty}\langle[\Delta x(t)]^2\rangle \to 2k_BT(m\eta_0)\,\tau_1/(1+\eta_0\tau_1)^2\,t^2$, and the coefficient of t^2 arrives at a maximum if $\tau_1 = 1/\beta_0$. Notice that the present noise differs

from the harmonic noise;[16] the latter is a narrow-band noise and is also called a quasi-colored noise, and its high-frequency part of the spectrum is declining. Moreover, the fractal noise proposed by Jung,[17] in particular, is an overdamped harmonic noise. Thus, they cannot induce a superdiffusion.

The dimensionless units, $k_B = 1.0$, $m = 1.0$, the time step $\Delta t = 10^{-3}$, and the trajectory number $N = 10^4$ are used in the calculations. In Fig. 1, we plot numerical results of the mean-square displacement of a free particle $\langle[\Delta x(t)]^2\rangle$. The error of the present algorithm related to theoretical data is less than one per cent. It is seen that $\langle[\Delta x(t)]^2\rangle$ is proportional to t^2 in the long-time limit when the noise is in the region of "green" noise.

Dependence of the mean-square displacement of the particle on the initial distribution of the broadband noise is shown in Fig. 2. It is seen that the numerical data diverges from the theoretical result if the temperature of the initial distribution is not chosen to be equal to the system temperature. This implies that velocity memory leads to a transition error being added and developed. Indeed, if the initial temperature $T_0 = 0$, the development of fluctuation will be very weak in the system.

Now we apply the proposed noise and algorithm to a periodically flashing ratchet. The potential is chosen to be a periodic sawtooth function as

$$U(x) = \frac{U_0}{(1-\alpha)\,L}\,x, \qquad 0 < x < (1-\alpha)\,L,$$

$$= \frac{U_0}{\alpha L}\,(L-x), \qquad (1-\alpha)\,L < x < L, \tag{15}$$

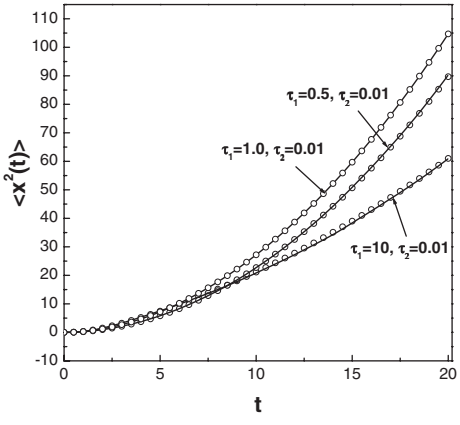

Fig. 1. The mean-square displacement of a free particle vs time for various τ_1 and τ_2 at the temperature $T = 1.0$. The solid lines and open circles are numerical and theoretical results, respectively.

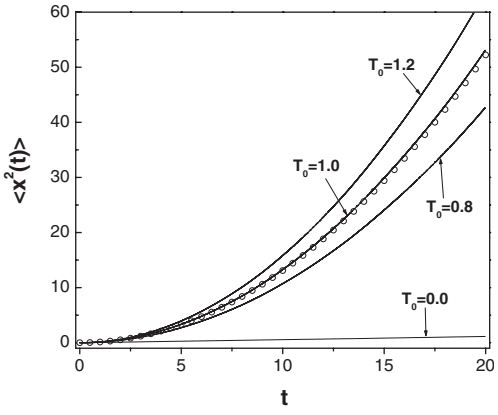

Fig. 2. Dependence of the mean-square displacement of a free particle on the initial temperature T_0. The parameters used are $T = 1.0$, $\tau_1 = 0.2$, and $\tau_2 = 0.02$. The solid lines and open circles are numerical and theoretical results, respectively.

where U_0, α, and L are the barrier height, asymmetrical parameter, and periodic length of the ratchet potential, respectively. The potential $U(x)$ is instead of $z(t)\,U(x)$ in Eq. (10),[18–20] and $z(t)$ is a periodic process taking two values: $z(t) = 1$ for $jt_p < t < (j+1)\,t_p$; $z(t) = 0$ for $(j+1)\,t_p < t < (j+2)\,t_p$, where t_p is the half-cycle period of the particle expressing the potential on and off.

Due to a strong velocity-memory effect in the presence of the thermal band-passing noise, the system requires a long time for arriving at the stationary state. We use two different ways to evaluate the mean velocity in the stationary state. If the mean velocity of the particle is large, it is determined numerically by $\langle v \rangle = \frac{1}{t_f - t_s} \int_{t_s}^{t_f} \langle v(t') \rangle\, dt'$, where t_s is the time of the system arriving at the stationary state and t_f is final time of the simulations. If the mean velocity is small, for instance, smaller than 10^{-2}, it is evaluated by $\langle v \rangle = \sum_{n=1}^{N} [x_n(t_f) - x(0)]/Nt_f$, N being the simulated trajectory number.

In Fig. 3, we show the mean velocity of the particle as a function of the half-cycle period t_p and compare it with the result of a white noise ($\tau_1 \to \infty$ and $\tau_2 \to 0$) at the same parameters $\alpha = 0.8$, $\beta_0 = 1.0$, and $T = 0.01$. The mechanism of directed motion can be understood well from the following facts. When the potential is off, the particle diffuses freely and symmetrically, and the particle crossing the position of the nearest barrier is larger than that of the farthest barrier. However, when the potential is recovered, the particle moves along two sawtooth sides of the ratchet potential, and it is easy for the particle to descend to the bottom of a well

along the steeper side of the potential. The magnitude and direction of the mean velocity of the particle will be determined by the competition between the above two processes. It is seen from Fig. 3 that, in the presence of thermal band-passing noise, the mean-velocity curve as a function of t_p has two peaks. The first peak corresponds to a maximum of the difference between forward and backward probabilities during a short cycle period, and the second peak is due to the particle having enough time to descend to the bottom of a well along two sawtooth sides of the ratchet potential, thus the particle can move neatly a long distance. Moreover, it is observed that the maximum of the mean velocity in the presence of thermal band-passing noise is much larger than that of the usual flashing ratchet at the same parameters.

The dependence of the mean velocity on the asymmetry of the ratchet potential is shown in Fig. 4. It is seen that, with decreasing asymmetry α of the ratchet potential, the first peaks of the mean velocity drift toward large t_p and their highs decrease. For a fast flashing-ratchet system, when the potential is off, the particle crosses the position of the nearest barrier more easily than the farthest barrier, and this possibly decreases with decreasing asymmetry of the ratchet; the difference between the right and left probabilities is also a decreasing function of α; thus the peak of the mean-velocity curve decreases. Moreover, the second peak of the mean-velocity curve does not appear for small α, because there does not exist an optimal t_p to make the probability drift $P_f - P_b$ become maximum when the flashing frequency of the ratchet is slow.

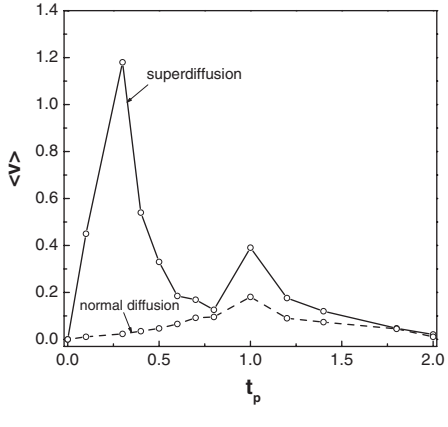

Fig. 3. The mean velocity as a function of the half period t_p at fixed asymmetrical parameter $\alpha = 0.8$ and temperature $T = 0.01$. The solid and dashed lines are the results of broadband noise ($\tau_1 = 0.5$ and $\tau_2 = 0.05$) and white noise, respectively.

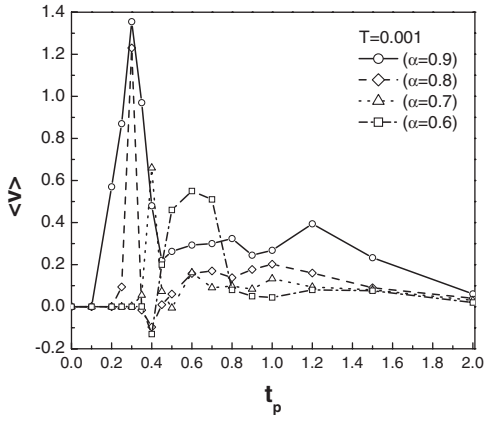

Fig. 4. The mean velocity as a function of t_p for several asymmetries α of the ratchet potential at a fixed temperature $T = 0.001$.

A plot of the mean velocity as a function of t_p for several values of T is shown in Fig. 5. As an interesting point, we note that the maximum of $\langle v \rangle$ increases with decreasing temperature and the curves of mean velocity for different values of T converge to a single peak; this behavior has been observed in the normal overdamped flashing ratchet;[20] however, as Astumian and Bier[19] have argued, no flows exist at $T = 0$.

The inertia effect is observed in Fig. 6. A finite inertia causes a complex mean-velocity behavior. A global maximum appears for finite mass, and hence finite inertia may enhance the value of the mean velocity, since the diffusion and mobility have a weaker effect on a larger mass.

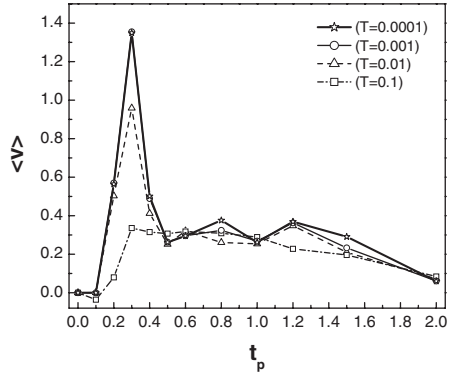

Fig. 5. The mean velocity as a function of t_p for different temperatures at a fixed $\alpha = 0.8$.

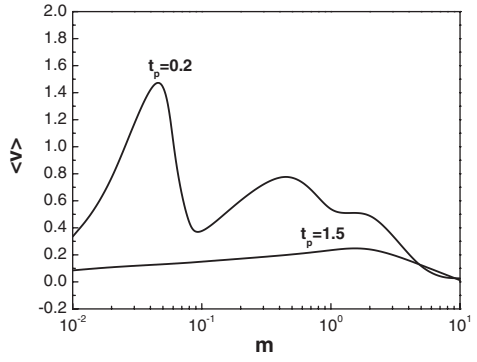

Fig. 6. The mean velocity as a function of t_p for several inertial masses m at fixed $T = 0.001$ and $\alpha = 0.9$.

4. SUMMARY

An accurate and fast comprehensive algorithm for numerically simulating a non-Markovian Langevin equation with a thermal band-passing noise is proposed; it is based on the closed integral approach for both damping and noise terms and the second-order Runge–Kutta method for nonlinear force. The correct initial distribution of the noise is presented and tested. Non-equilibrium transport in a flashing-ratchet potential subject to the thermal band-passing noise is considered. The results show that there are two peaks for the mean velocity as a function of the half-cycle period for a large asymmetrical ratchet. Moreover, the maximum of the mean velocity in the superdiffusive flashing ratchet is much larger than that in the usual flashing ratchet. Finite inertia can enhance the mean velocity and the directed flux reversals in the underdamped case. These phenomena can be understood well from diffusion and mobility of the particle in the potential on and off during a cycle period. It is believed that the present band-passing colored noise and numerical algorithm for simulating non-Markovian Langevin equations should have numerous applications.

ACKNOWLEDGMENTS

This work was supported by the National Natural Science Foundation of China under Grant No. 10075007.

REFERENCES

1. For a review, see R. Metzler and J. Klafter, *Phys. Rep.* **339**:1 (2000).
2. A. Mauger and N. Pottier, *Phys. Rev. E* **65**:056107 (2002).

3. E. Lutz, *Phys. Rev. E* **64**:051106 (2001); *Europhys. Lett.* **54**:293 (2001).
4. R. Metzler and I. M. Sokolov, *Europhys. Lett.* **58**:482 (2002); R. Metzler and J. Klafter, *Phys. Rev. E* **61**:6308 (2000).
5. R. Morgado, F. A. Oliveira, G. G. Batrouni, and A. Hansen, *Phys. Rev. Lett.* **89**:100601 (2002).
6. H. Scher, M. F. Shlesinger, and J. T. Bendler, *Phys. Today* **44**:26 (1991); M. F. Shlesinger, G. M. Zaslavsky, and J. Klafter, *Nature* **363**:31 (1993); T. Srokowski, *Phys. Rev. Lett.* **85**:2232 (2000).
7. J. D. Bao and S. J. Liu, *Phys. Rev. E* **60**:7572 (1999).
8. For a recent review, see P. Reimann, *Phys. Rep.* **361**:57 (2002).
9. S. A. Guz, I. G. Rusavin, and M. V. Sviridov, *Phys. Lett. A* **274**:104 (2000); S. A. Guz and M. V. Sviridov, *Chaos* **11**:605 (2001).
10. T. Munakata and T. Kawakatsu, *Prog. Theor. Phys.* **74**:262 (1985).
11. J. D. Bao and Y. Z. Zhuo, *Phys. Lett. A* **239**:228 (1998).
12. J. D. Bao, *J. Stat. Phys.* **99**:595 (2000).
13. R. L. Honeycutt, *Phys. Rev. A* **45**:604 (1992).
14. R. Mannella and V. Palleschi, *Phys. Rev. A* **40**:3381 (1989).
15. R. F. Fox, *Phys. Rev. A* **43**:2649 (1991).
16. L. Schimansky-Geier and Ch. Zülicke, *Z. Phys. B* **79**:41 (1990); M. I. Dykman and R. Mannella, *Phys. Rev. E* **47**:3996 (1993); S. J. B. Einchcomb and A. J. McKane, *Phys. Rev. E.* **49**:259 (1994).
17. P. Jung, *Phys. Rev. E* **50**:2513 (1994); *Phys. Lett. A* **207**:93 (1995).
18. L. P. Faucheux, L. S. Bourdieu, P. D. Kaplan, and A. J. Libchaber, *Phys. Rev. Lett.* **74**:1504 (1995).
19. R. D. Astumian, *Science*, **276**:917 (1997); R. D. Astumian and M. Bier, *Phys. Rev. Lett.* **72**:1766 (1994).
20. A. Mielke, *Ann. Phys.* **4**:721 (1995).
21. J.-F. Chauwin, A. Ajdari, and J. Prost, *Europhys. Lett.* **32**:373 (1995); J. D. Bao, *Phys. Lett. A* **267**:122 (2000).
22. B. Lindner, L. Schimansky-Geier, P. Reimann, P. Hänggi, and M. Nagaoka, *Phys. Rev. E* **59**:1417 (1999).